SETAC PRESS

Environmental Toxicology and Chemistry, Vol. 19, No. 9, pp. 2224–2234, 2000

Printed in the USA
0730-7268/00 $9.00 + .00

EFFECT OF MASS-TRANSFER LIMITATIONS ON BIOAVAILABILITY OF SORBED NAPHTHALENE IN SYNTHETIC MODEL SOIL MATRICES

HENDRICUS MULDER,†‡ ANTON M. BREURE,*† JOHAN G. VAN ANDEL,† J. TIM C. GROTENHUIS,‡ and WIM H. RULKENS‡

†Laboratory for Ecotoxicology, National Institute for Public Health and the Environment, P.O. Box 1, 3720 BA Bilthoven, The Netherlands
‡Department for Environmental Technology, Wageningen Agricultural University, P.O. Box 8129, 6700 EV Wageningen, The Netherlands

(*Received* 17 *August* 1999; *Accepted* 8 *February* 2000)

Abstract—External and internal mass-transfer resistances influencing the bioavailability of sorbed naphthalene in a synthetic model matrix for soil aggregates were investigated in batch experiments in mixed reactors. Amberlite® adsorption resins (XAD4 and XAD7) were used as the synthetic model for soil aggregates. The effect of hydrodynamic conditions in the slurry phase on the diffusive transport across a stagnant film surrounding the model particles was studied. In addition, a mechanistic model was developed based on mass balances, diffusion equations, a nonlinear sorption isotherm, and microbial degradation kinetics. Experimental results could be explained well with this model. In the absence of external transfer limitations, intraparticle effective diffusion coefficients of $(3.55 \pm 0.10) \times 10^{-9}$ m²/s and $(5.29 \pm 0.86) \times 10^{-10}$ m²/s were determined for naphthalene in Amberlite XAD4 and XAD7, respectively.

Keywords—Bioavailability Biodegradation Sorption Modeling Naphthalene

INTRODUCTION

The biological remediation of soils polluted with polycyclic aromatic hydrocarbons (PAHs) is considered an attractive alternative to the more destructive physical and chemical sanitation techniques. The biological value of the soil is preserved and, therefore, the soil can be brought back into the environment, whereas soil treated otherwise is often dumped at waste disposal sites or only has a limited application as construction material.

However, major drawbacks exist in bioremediation that limit its application. Because biological processes are used to lower pollutant concentrations, biodegradation of the contaminants must be possible by the microbial population present and environmental conditions have to allow for a sufficient biodegradation capacity of this population. In addition, biodegradation of noncontaminant compounds (soil organic matter) or the presence of other contaminants should not inhibit the conversion process. In the case of PAHs that are located in the soil under former gaswork plants, cyanide pollution, for instance, may limit the potential of bioremediation.

But even if the pollutants can be metabolized by the bacteria or fungi and copollution does not affect this conversion, low degradation rates can occur. The slow release of PAHs from the soil constituents to the aqueous phase is proven to be limiting for the overall biodegradation rate in many cases [1]. Low mass-transfer rates caused by strong sorptive interactions with soil organic matter and intraparticle diffusion limitations are responsible for the low bioavailability of PAHs in soil [2–8].

When studying the limited bioavailability of PAHs in soil, a complex heterogeneous system is under investigation in which various physicochemical parameters are undefined. This heterogeneity occurs in both textural as well as in structural features of soil material. Therefore, soil matrices should be well characterized in order to obtain a qualitatively as well as a quantitatively sound description of the processes involved. An alternative approach is the use of synthetic matrices as model constituents of soil that possess defined homogeneous properties [7,9–14]. Using these model systems, the processes determining the reduced bioavailability of sorbed PAHs can be simulated and modeled. Obviously, the physicochemical properties of the model system must be similar to the soil type under investigation so that results can be translated to realistic systems [10].

A reduced bioavailability of PAHs mainly occurs in fine-textured soils such as silt and clay and in organic matter fractions. This is due to relatively high specific surface areas and the relatively slow rate of aqueous diffusion through the soil particle matrix and in water-saturated clay aggregates as a result of constrictivity and tortuosity effects. Therefore, model systems must consist of porous matrices in which sorption of the contaminants to an organic hydrophobic phase is possible and in which mass-transfer resistances can be rate-limiting to the overall release rate from the particles.

The particle diameter is an important factor when studying mass-transfer processes in aggregates. However, because of the heterogeneity of soil material, employing defined size limits for soil aggregates is impossible. Although literature exists on particle texture and structure, this literature stems from agricultural sources and often focuses on macroaggregate properties [15–18]. However, in bioremediation practice, the effluent of a classification treatment installation is mainly what is considered for further clean-up. This effluent consists of microaggregates [19] that contain high amounts of clay particles and organic matter.

The purpose of this study was to investigate the mutual influence of intra-aggregate mass-transfer processes and microbial degradation of naphthalene in synthetic model soil ma-

* To whom correspondence may be addressed (ton.breure@rivm.nl).

Table 1. Physical properties of the sorbent used as synthetic model soil (from supplier data unless stated otherwise)

Sorbent	Average pore diameter (nm)	Specific surface area (m^2/g)	Skeletal density (kg/m^3)	Porosity[a] (m^3/m^3)
XAD4	4.0	725	1,080	0.71
XAD7	9.0	450	1,240	0.78

[a] [35].

trices. These model soil systems were used to validate a mathematical model developed to describe the biological processes and the mass-transfer phenomena. Although several mechanistic models have been presented earlier in the literature, this work was aimed at the incorporation of external mass transfer and internal mass transfer, nonlinear sorption processes, and nonlinear biodegradation kinetics into one model. The combination of these specific aspects in one model and the experimental validation with model systems provide a new methodology that can increase the insight in the limited bioavailability of hydrophobic soil pollutants. Because of the mechanistic nature of the mathematical model, reasonable predictions with respect to the fate and behavior of other compounds in soil matrices can be made.

MATERIALS AND METHODS

Bacterial cultures

In previous investigations [7], the isolation of the gram-negative *Pseudomonas* strain 8909N (DSM-No. 11634) was described. This organism can use naphthalene as the sole carbon and energy source.

Media and culture conditions

A buffered mineral medium with pH 7.0 was used in the experiments [12]. Both the physicochemical and the biodegradation experiments were conducted at 30°C to ensure similar conditions.

Synthetic soil matrix

Commercially available Amberlite XAD4 and XAD7 resins (Supelco, Bellefonte, PA, USA) were used as porous matrices. The physical properties of these materials are shown in Table 1. The XAD was sieved (Endecotts, Keison Products, Chelmsford, UK) and the resulting size fractions (425–500 μm; 500–600 μm; 710–850 μm; 850–1,000 μm; 1,000–2,360 μm) were stored at 4°C in rubber-stoppered serum flasks. Contamination of the matrices with naphthalene was performed in 250-ml serum flasks supplemented with 200 ml of medium and approximately 50 g of Amberlite resin. Naphthalene was melted in stainless steel cups with conical-shaped notches [12] at a temperature of 100°C, after which the melts were cooled at room temperature. This procedure resulted in smooth melts with specified surface areas of 3.14×10^{-4} m^2, which were amended to the serum flasks. After a certain period, the stainless steel cups with the solid PAH were removed and the XAD particles were separated from the aqueous solution by filtration.

Sorption isotherms

Adsorption and desorption isotherms were determined under sterile conditions at 30°C in 100-ml serum flasks with Teflon®-lined stoppers. Gravimetrically determined amounts of loaded and unloaded XAD, respectively, were suspended in 90 ml of medium without naphthalene or in naphthalene solutions. After a period of 7 d, naphthalene liquid-phase concentrations were determined by high-performance liquid chromatography (HPLC) analysis. This period was long enough to assure equilibrium conditions.

Dynamic sorption and biodegradation experiments

Dynamic experiments were performed in slurry reactors of 500 ml (d_i = 0.024 m) [12] and of 1,500 ml (d_i = 0.045 m; Applikon, Schiedam, The Netherlands) with disc-mounted flat-blade turbine impellers at 30°C, where d_i is the impeller diameter (m). Particle-free solutions (stainless steel inlet filter, 10-μm porosity; Alltech, Deerfield, IL, USA) were pumped through quartz cuvets in which absorption at 276 nm (A_{276}) and at 540 nm was measured at discrete time intervals (Varian Cary 1 [500-ml reactor], Palo Alto, CA, USA; Perkin Elmer Lambda 15 [1,500-ml reactor], Norwalk, CT, USA) with mineral medium as reference. Stainless steel and Viton (GLB, South El Monte, CA, USA) tubing was used to interconnect the reactor, pump, and spectrophotometer. Before the experiments, the reactors were autoclaved (20 min at 120°C) and tubing was sterilized by successively recirculating solutions of 1 M NaOH, 1 M HCl, and sterile mineral medium for 30 min each [12]. At the start of an experiment, XAD particles were added to the reactor and naphthalene concentrations in the liquid phase were measured until equilibrium was reached. In the case of biodegradation experiments, bacteria were subsequently inoculated to these reactors by pipeting 0.5 ml of an active culture suspension in the reactors. In order to prevent interference of light scattering by bacteria on the spectrophotometric determination of the naphthalene concentration, samples were drawn from the recirculating fluid by a three-way valve after inoculation. Samples were filtered over 0.22-μm rotrand filters (Schleicher & Schuell, Dassel, Germany) to remove bacteria and were directly prepared for HPLC analysis.

Analytical procedures

Biomass formation was determined by measuring optical density at 540 nm (OD_{540}) in the flow-through cuvette. The OD_{540} values were converted to biomass concentrations by determining the protein concentration at a certain optical density (conversion factor 4.33×10^{-1} $kg/m^3/U$ OD_{540}) [12]. Dissolved naphthalene concentrations were determined by HPLC (Hewlett-Packard series HP 1050, Avondale, PA, USA) and by on-line spectrophotometric measurements. The HPLC samples were 50% diluted with acetonitrile and were injected on a 20-cm Chromspher C_{18}-PAH column (Chrompack, Middelburg, The Netherlands) with a 88:12 (v/v) mixture of acetonitrile and water as eluent. Naphthalene concentrations were detected by an ultraviolet detector at 276 nm. The experimental setup used for the on-line spectrophotometric determination of dissolved naphthalene concentrations was described earlier [12]. A molar absorption coefficient of 5.45×10^3/M/cm was determined and used to convert A_{276} values to dissolved naphthalene concentrations. Initial loadings of the resins were determined by extraction with acetonitrile in 100-ml serum flasks from which HPLC samples were drawn after 24 h. The dry weight of the XAD was determined gravimetrically after 24 h of drying at 100°C.

MODELING

The sorption equilibrium of naphthalene to Amberlite resins is described by the Freundlich isotherm, which gives the nonlinear relationship between the naphthalene concentration in the sorbed phase and the dissolved naphthalene concentration in the pore liquid

$$Q = K_F C^n \tag{1}$$

where Q is the sorbed naphthalene concentration (kg/kg), K_F is the Freundlich sorption coefficient (m^{3n}/kg^n), C is the dissolved naphthalene concentration (kg/m^3), and n is a dimensionless constant. When the natural logarithm of Q is plotted versus the natural logarithm value of C, a straight line is obtained with a slope equal to n and an intercept of the vertical axis equal to the natural logarithm of K_F.

The release of contaminant from a porous particle is a dynamic process, which can be modeled by setting up a mass balance for a specific geometry and the substitution of a diffusion equation [20]. Assuming a spherical shape of the Amberlite resins, a concentration-independent diffusion coefficient in the pore liquid, and instantaneous local equilibrium at a certain location in the porous particle, Equation 2 describes the variation of concentration in time as a function of the concentration gradient in the particle at a given location

$$\frac{\partial C}{\partial t}\varepsilon + \frac{\partial Q}{\partial t}(1 - \varepsilon)\rho_s = D_{eff}\left(\frac{\partial^2 C}{\partial r^2} + \frac{2}{r}\frac{\partial C}{\partial r}\right) \tag{2}$$

where ε is the particle volumetric porosity (m^3/m^3), t is the time (s), ρ_s is the skeletal density of the solid phase (kg/m^3), D_{eff} is the effective diffusion coefficient through the porous matrix (m^2/s), and r is the distance from the center of the particle (m). The effective diffusion coefficient is defined as the binary diffusion coefficient of the PAH in dilute water solutions corrected for tortuosity and constrictivity effects imposed on this coefficient by the matrix geometry by means of a lumped matrix factor (κ) [8,21]

$$D_{eff} = \frac{\varepsilon D_{AB}}{\kappa} \tag{3}$$

where D_{AB} is the binary diffusion coefficient of the PAH in dilute aqueous solutions and κ is the dimensionless matrix factor. By substitution of Equation 1 into Equation 2 the following equation is obtained

$$\frac{\partial C}{\partial t} = \frac{D_{eff}}{\varepsilon + (1 - \varepsilon)\rho_s K_F n C^{(n-1)}}\left(\frac{\partial^2 C}{\partial r^2} + \frac{2}{r}\frac{\partial C}{\partial r}\right) \tag{4}$$

In most studies that use radial diffusion models to describe the behavior of hydrophobic compounds in soil particles an overall effective diffusion coefficient is defined [4,8,22]. Although these overall diffusion coefficients were defined for the case of a linear isotherm (e.g., $n = 1$ in Eqn. 1), we follow a similar definition

$$D^o_{eff} = \frac{D_{eff}}{\varepsilon + (1 - \varepsilon)\rho_s K_F n C^{(n-1)}} \tag{5}$$

where D^o_{eff} is the overall effective diffusion coefficient (m^2/s). Equation 4 can be simplified by introducing the following normalized parameters

$$\xi = \frac{r}{R} \tag{6}$$

$$\tau = \frac{tD_{eff}}{R^2} \tag{7}$$

where ξ is the dimensionless normalized location in the particle, R is the radius of the particle (m), and τ is the dimensionless normalized time. Substitution of the normalized parameters (Eqns. 6 and 7) in Equation 4 yields

$$\frac{\partial C}{\partial \tau} = \frac{1}{\varepsilon + (1 - \varepsilon)\rho_s K_F n C^{(n-1)}}\left(\frac{\partial^2 C}{\partial \xi^2} + \frac{2}{\xi}\frac{\partial C}{\partial \xi}\right) \tag{8}$$

The boundary conditions for Equation 8 follow from the definition of a zero concentration gradient in the center of the particle (boundary condition I [BC I]) and the condition that the mass flux from the surface of the particle equals the mass flux through the laminar layer (BC II). In addition to intraparticle mass-transfer resistances, diffusion across a stagnant liquid film surrounding the particle influences the overall transfer rate to a well-mixed aqueous phase [20]. This additional mass-transfer resistance can be modeled by assuming a linear concentration gradient across the laminar liquid film and thus defining the mass flux through the film as

$$N = \varepsilon k_\ell (C_{\xi=1} - C_b) \tag{9}$$

where N is the mass flux through the laminar layer ($kg/m^2/s$), k_ℓ is the mass-transfer coefficient of the naphthalene (m^2/s), and C_b and $C_{\xi=1}$ are the concentrations in the mixed bulk liquid and at the interface of the particle with the laminar layer, respectively (kg/m^3). The boundary conditions (BCs) and initial condition (IC) for Equation 8 are therefore

$$\left.\frac{\partial C}{\partial \xi}\right|_{\xi=0} = 0 \qquad \text{BCI} \tag{10}$$

$$-D_{eff}\left.\frac{\partial C}{\partial \xi}\right|_{\xi=1} = \varepsilon k_\ell R(C_{\xi=1} - C_b) \quad \text{BCII} \tag{11}$$

with

$$C = C_i \quad \text{for } 0 \geq \xi \geq 1;$$

$$C_b = 0 \quad \text{at } \tau = 0 \quad \text{IC (desorption)} \tag{12}$$

$$C = 0 \quad \text{for } 0 \geq \xi \geq 1;$$

$$C_b = C_i \quad \text{at } \tau = 0 \quad \text{IC (adsorption)} \tag{13}$$

where C_i is the initial dissolved naphthalene concentration (kg/m^3). In the case of desorption, this concentration is in equilibrium (Eqn. 1) with the initial sorbed naphthalene concentration Q_i (kg/kg). The magnitude of the mass-transfer coefficient over the laminar film (k_ℓ) depends on the flow conditions imposed by shaking or stirring. The external mass transfer can be characterized by the dimensionless Sherwood number (Sh)

$$Sh = \frac{2Rk_\ell}{D_{AB}} \tag{14}$$

The relationship between reactor flow conditions and the external mass transfer is often described as a function of the dimensionless Reynolds and Schmidt numbers

$$Sh = 2 + \alpha Re^\beta Sc^\gamma \tag{15}$$

$$Re = \frac{2\rho_\ell v R}{\eta} \tag{16}$$

$$Sc = \frac{\eta}{\rho_\ell D_{AB}} \tag{17}$$

where Re and Sc are the dimensionless Reynolds and Schmidt numbers, respectively. The parameter ρ_ℓ is the liquid density

(kg/m^3), v is the relative velocity of the particle to the liquid (m/s), and η is the dynamic viscosity of the liquid phase (kg/m/s). The constants α, β, and γ are dimensionless and have values of 0.60, 0.5, and 0.33, respectively, for mixed slurries of spherical particles [23,24]. However, determination of the dimensionless Reynolds number requires information on the relative velocity of the particles to the fluid (v), which is difficult to obtain. Although alternative formulations exist for the Reynolds number as a function of the energy dissipation rate to the liquid phase by means of mixing, these relations have a limited applicability [23]. Therefore, in this study, only the impeller Reynolds number is used to evaluate whether turbulent conditions exist in the stirred vessel [24]

$$Re_i = \frac{\rho_\ell S_i d_i^2}{\eta} \tag{18}$$

where Re_i is the impeller dimensionless Reynolds number, S_i is the rotational speed of the impeller (s^{-1}), and d_i is the diameter of the impeller (m). At high Re_i values ($Re_i > 10{,}000$) the flow in the vessel is considered turbulent throughout the entire liquid phase. Between Reynolds numbers of 10 to 10,000, the flow is turbulent at the impeller and might be laminar at distant locations in the vessel. Below Reynolds numbers of 10 the flow is considered laminar in the complete liquid phase.

To determine whether external or internal mass transfer is limiting the overall release or uptake rate of naphthalene, the dimensionless Biot number (Bi) can be used [3,24]

$$Bi = \frac{k_\ell R}{D_{eff}} \tag{19}$$

At high Biot numbers ($Bi \gg 1$) external diffusion limitations can be neglected and intraparticle mass transfer is rate-determining. At low Biot numbers ($Bi \ll 1$) the external mass-transfer resistances dominate the overall transfer process.

Bacteria have dimensions in the order of micrometers [25] and, therefore, are unable to penetrate the pores of the porous particles, which have an average pore size of nanometers, as is the case for the XAD particles (Table 1). Therefore, biodegradation can only occur in the liquid phase. When the biodegradation in the stagnant layer is neglected, the following mass balance can be postulated to describe the change in the dissolved PAH concentration in time in the bulk liquid phase

$$\frac{dC_b}{dt} = \frac{\varepsilon k_\ell A}{V}(C_{\xi=1} - C_b) - \frac{\mu X}{Y} \tag{20}$$

where V is the volume of the liquid phase per particle (m^3), A is the particle external surface area (m^2), μ is the growth rate of the bacteria (s^{-1}), X is the biomass concentration (kg/m^3), and Y is the yield of the organisms on the PAH (kg/kg). When adsorption or desorption experiments under sterile conditions were modeled, the biomass concentration was set to zero for the duration of these sterile conditions. The initial conditions for Equation 20 are given in Equations 12 or 13. The volume per particle is calculated on the basis of the following equation:

$$V = \frac{V_R \frac{4}{3}\pi R^3 (1 - \varepsilon)\rho_s}{m_s} \tag{21}$$

where V_R is the total liquid volume in the reactor (m^3) and m_s is the total dry weight of the particles in the reactor (kg). The volume of the water inside the pores was neglected. The change in biomass concentration in time can be modeled by

$$\frac{dX}{dt} = \mu X \quad \text{with} \tag{22}$$

$$X = 0 \qquad \text{for } t < t_I \tag{23}$$

$$X = X_I \qquad \text{for } t = t_I \tag{24}$$

where X_I is the biomass concentration (kg/m^3) at the moment of inoculation t_I (s). The growth rate of the bacteria is modeled by assuming Monod kinetics for the growth on dissolved naphthalene [12]

$$\mu = \mu_{max}\frac{C}{C + K_s} \tag{25}$$

where μ_{max} is the maximum growth rate of the bacteria (s^{-1}) and K_s is the Monod constant (kg/m^3). From Equations 22 and 25, zero-order growth can be deduced to occur at relatively high PAH concentrations compared to the Monod constant, and that first-order growth occurs at relatively low concentrations. To assess whether the biodegradation in the laminar layer may be neglected the dimensionless Hatta number (Ha) is defined at first-order growth conditions [24]

$$Ha = \frac{\sqrt{D_{AB}\left(\frac{\mu_{max} X}{Y K_s}\right)}}{k_\ell} \tag{26}$$

At low Hatta numbers ($Ha < 0.3$) and for a relatively low volume of the boundary layer compared to the liquid volume (V), the biodegradation in the laminar boundary layer can be neglected. At high Hatta numbers ($Ha > 3$), a significant reaction rate occurs in the boundary layer and Equation 9 is no longer valid. This becomes important at high biomass concentrations and low mass-transfer coefficients.

In order to calculate the development of biomass (X) and bulk liquid PAH concentrations (C_b) in time, the set of coupled differential equations formed by Equations 8, 20, and 22 has to be solved. Because of the nonlinearity of the bacterial transformation kinetics and of the Freundlich isotherm, the set of differential equations cannot be integrated analytically and numerical integration methods are necessary to approximate the solution. A Crank–Nicholson scheme is the recommended discretization scheme to transform the set of differential equations into a set of j linear equations with j unknowns [26]. The value of j is determined by the number of locations at which the dissolved concentration (C) is evaluated. A Euler integration method is applied to calculate the evolution of biomass concentration in time.

The description of the experimental data by the model was optimized in a two-step procedure. First, the mass transfer was quantified by determination of the effective diffusion coefficient (D_{eff}) and the mass-transfer coefficient (k_ℓ) from sterile desorption and adsorption experiments. In the second step, the microbial parameters were quantified by determining the maximum growth rate (μ_{max}) and the yield (Y) from the biodegradation experiments. The value of the effective diffusion coefficient was optimized by minimizing a chi-squared function [26] at negligible external mass-transfer resistances

$$\chi^2 = \sum_{z=1}^{Z} [C_z|_\tau - C(\tau)]^2 \tag{27}$$

where χ^2 is a dimensionless parameter, z is the identifier of the experimental individual data points, Z is the total number of experimental data points, $C_z|_\tau$ is the experimental PAH concentration at time τ, and $C(\tau)$ is the concentration at time τ predicted by the model. At low energy dissipation rates, the value of the effective diffusion coefficient (D_{eff}) as determined from the above-mentioned calculations was introduced as a fixed parameter. The value of the mass-transfer coefficient (k_ℓ) was subsequently optimized by minimizing χ^2 in Equation 27. Thereafter, the value of the maximal growth rate of the bacteria was determined from the exponential growth phase by a procedure that was also adapted in earlier work [12]. In this procedure the natural logarithm of the ratio of the biomass concentration over the initial biomass concentration is calculated. Then, this logarithmic value is plotted against time. In the growth phase where zero-order kinetics are valid, a straight line is obtained and the slope of this line equals the maximum growth rate of the bacteria. Finally, the value of the yield coefficient was optimized in the biodegradation phase ($t = t_l$) by minimizing another chi-squared function

$$\chi^2 = \sum_{z=1}^{Z} [X_z|_\tau - X(\tau)]^2 \quad (28)$$

where $X_z|_\tau$ is the experimental biomass concentration at time τ (kg/m^3) and $X(\tau)$ is the concentration at time τ predicted by the model (kg/m^3). The values of χ^2 were minimized by applying a bracketing method [26].

RESULTS

Sorption isotherms

Sorption isotherms of naphthalene on Amberlite XAD4 and XAD7 were determined under sterile conditions at a temperature of 30°C in mineral medium (Fig. 1) and Freundlich isotherms were fitted through the experimental data. Results of these fits are given in Table 2. Adsorption and desorption isotherms were identical so the sorption of naphthalene to both sorbents was reversible.

Mass-transfer parameters

One of the most important parameters in the current model is the effective diffusion coefficient of naphthalene in the porous Amberlite matrices. This parameter can be determined by measuring the amount of naphthalene that is taken up by an Amberlite particle or the amount that is released from a homogeneously contaminated particle in course of time. To be sure that external mass-transfer limitations are negligible during these measurements, information must be generated on the influence of reactor hydrodynamics on these external resistances [27]. Therefore, dynamic sorption experiments were conducted with the resins at different liquid mixing rates. Adsorption experiments with uncontaminated resins and desorption experiments with naphthalene-contaminated XAD4 and XAD7 were performed in two different types of impeller-mixed reactors under aseptic conditions.

The adsorption tests were initiated by immersing a certain mass of a sieve fraction of the sorbent in an aqueous naphthalene solution. Subsequently, the decrease in the dissolved naphthalene concentration was followed by means of on-line spectrophotometric measurements at discrete time intervals. In the desorption tests, artificially polluted resin was brought into the water phase of the reactor and the increase in the dissolved naphthalene concentration was followed in time by the same analytical procedure. Pilot experiments showed that the loss of naphthalene due to adsorption to the apparatus was negligible, which was achieved by the use of glass vessels and Viton and stainless steel materials to interconnect the measuring equipment.

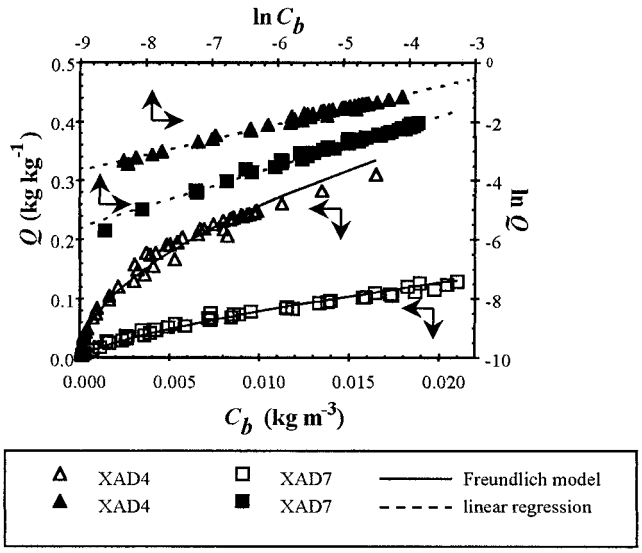

Fig. 1. Sorption isotherms of naphthalene to XAD4 and XAD7 Amberlite® resins. The closed symbols are the natural logarithmic values of the sorbed naphthalene concentration (Q) and the dissolved naphthalene bulk liquid concentration (C_b).

Results of sterile adsorption and desorption experiments with XAD7 are shown in Figure 2. From this figure, the desorption rate clearly increases with the rotational speed up to a rate of 1.67/s and then remains constant, indicating intraparticle diffusion being rate-limiting under those circumstances. From these and additional experiments, the external mass-transfer resistances were found to be negligible at rotational speeds above 1.2/s. In the range of rotational speeds applied, calculated impeller Reynolds numbers (Re_i) ranged from 4.2 $\times$ 10^2 to 3.3 $\times$ 10^4 (ρ_ℓ = 1 $\times$ 10^3 kg/m^3; η = 8.09 $\times$ 10^{-4} kg/m/s [24]). From the desorption and adsorption experiments at sufficiently high mixing rates, effective diffusion coefficients were determined for naphthalene in XAD4 and XAD7 pores (Table 2). Matrix factors (κ) for both types of sorbents were calculated on the basis of the effective diffusion coefficients according to Equation 3, and these are given in Table 2.

Desorption and subsequent biodegradation

The purpose of this work was to study the mutual influence between the mass-transfer processes of naphthalene, initially sorbed in porous particles, and the biodegradation of desorbed naphthalene outside these particles by bacteria. In earlier work,

Table 2. Freundlich sorption parameters (K_F, n) and intraparticle effective diffusion coefficients (D_{eff}) and matrix factors (κ) for the Amberlite resins. Calculation of the matrix factor from the value of D_{eff}, a value of 8.28 $\times$ 10^{-10} m^2/s, was used for the binary diffusion coefficient of naphthalene in water (D_{AB}) [40]

Sorbent	K_F (m^{3n}/kg^n)	n	D_{eff} (m^2/s)	κ
XAD4	2.89	0.53	(3.55 $\pm$ 0.10) $\times$ 10^{-9}	0.17
XAD7	1.93	0.69	(5.29 $\pm$ 0.86) $\times$ 10^{-10}	1.22

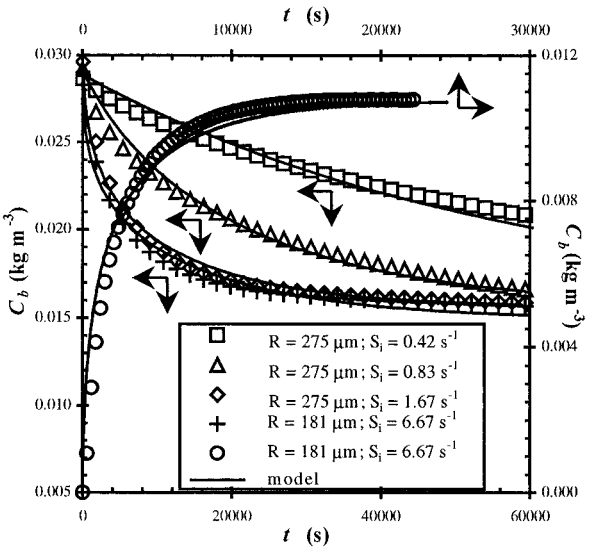

Fig. 2. Dynamic batch adsorption and desorption experiments with two different size fractions of Amberlite® XAD7. Experimental data indicated by symbols; drawn lines are model calculations. Adsorption experiments were conducted at different rotational speeds to investigate the presence of external mass-transfer resistances. Experiments shown were carried out in the 1,500-ml reactors with a 1,000-ml working volume (V_R).

a procedure was developed to quantify both the physicochemical process and the biodegradation of the released PAH in single-run experiments [12]. Although those experiments were conducted with solid-phase naphthalene, a similar approach was adapted in the experiments described in this section.

In the experiments the mass-transfer parameters first were determined in an aseptic phase (e.g., $X = 0$). Then the reactor was inoculated (at $t = t_I$) with bacteria (with $X = X_I$) to study the effect of the mass transfer on the biodegradation process. The aseptic part of the experiments was identical to the experiments described in the foregoing section. In the ideal situation, equilibrium with respect to the desorption process was established before inoculation. Thereafter, bacteria were added and the biomass concentration was measured on-line at discrete time intervals by a spectrophotometer. Because the biomass interferes with the spectrophotometric determination of dissolved naphthalene in the bulk of the liquid, samples were drawn from the reactor liquid for HPLC analysis after the moment of inoculation. Results of such an experiment are given in Figure 3A, showing the desorption of naphthalene from XAD7 particles and the subsequent biodegradation by *Pseudomonas* 8909N. These data have been described by the mathematical model and the values for the model parameters are given in Table 3. The value of the Monod constant ($K_s = 4.0 \times 10^{-5}$ kg/m^3) for naphthalene was determined in earlier reports on *Pseudomonas* 8909N [28].

Figure 3A shows the two-stage setup of the experiments. After the preloaded XAD7 was added to the reactor, dissolved naphthalene concentrations were measured by ultraviolet adsorption at 276 nm. At the moment where equilibrium was achieved, bacteria were added to the reactor medium and light scattering at 540 nm was now measured as a measure for the biomass concentration. Additional HPLC samples were drawn to determine the decrease in dissolved naphthalene concentrations. The maximum growth rate was determined from the slope of the $\ln(X/X_0)$ values at the exponential growth phase (Table 3). At the end of the experiment some colorization of

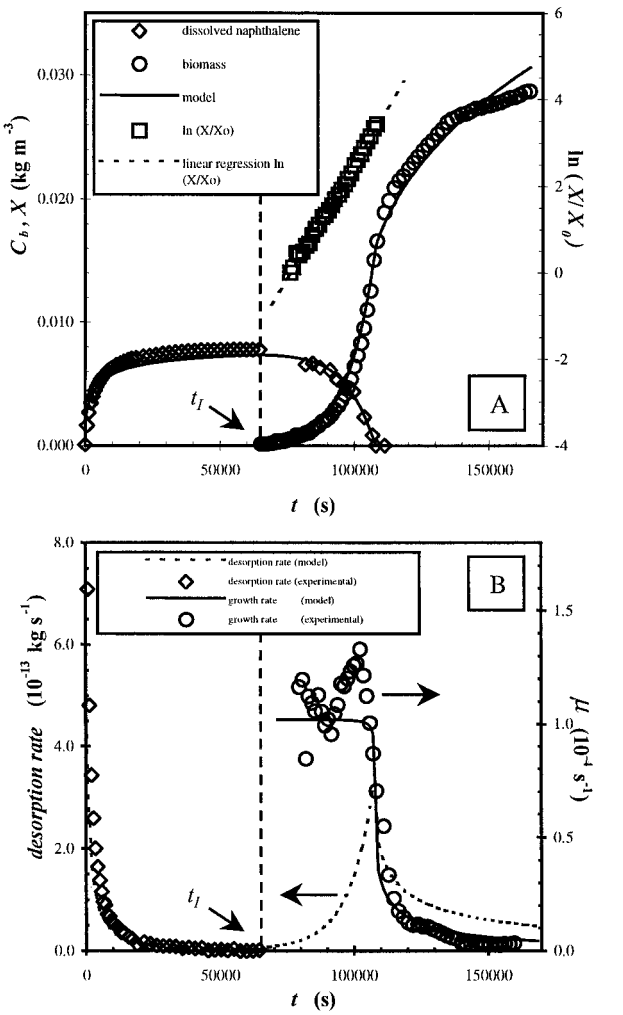

Fig. 3. (**A**) Desorption of naphthalene from XAD7 (1,000–2,360 μm) under aseptic conditions and the subsequent biodegradation of desorbed naphthalene by *Pseudomonas* 8909N. The natural logarithm plot is provided to illustrate the procedure to determine the maximum growth rate in the exponential growth phase. Symbols indicate experimental data and drawn lines are model calculations. The vertical dashed line indicates the moment of inoculation (t_I). The values of the parameters applied in the model calculations are provided in Table 3. (**B**) Experimental and calculated desorption rates of naphthalene from XAD7 particles (1,000–2,360 μm) and experimental and calculated growth rates in the biodegradation phase (Fig. 3A). The conditions of this experiment and the model parameters used to calculate the model lines are given in Table 3. The vertical dashed line indicates the moment of inoculation (t_I).

the originally white XAD7 was observed. The yellow-brown color was attributed to sorbed bacteria or metabolites in the medium. No quantification was performed on the amount of biomass that was sorbed to the surface of the XAD7.

From the results presented in Figure 3A, experimental desorption rates in the aseptic phase were calculated by dividing the increase in dissolved naphthalene concentration by the time interval in which this increase had occurred and multiplying by the volume of liquid per particle (V). Furthermore, growth rates were calculated in the biodegradation phase of the experiment by dividing the increase in biomass concentration in a certain time interval by this interval and by the current biomass concentration (Eqn. 22).

As in earlier work [12], significant scattering in the values of the maximum growth rate occurred at low biomass con-

Table 3. Experimental conditions and values of parameters used in the model calculations. A dash in the cells of the table indicates that these data are provided in the figure itself. To differentiate between fixed parameter values and parameters that were optimized on the basis of experimental data, an [a] or [b] is added above the parameter values, respectively

Parameter		Figure							
		3	4	5	6	7A	7A	7A	7A
S_i	(s^{-1})	1.67[a]	13.3[a]	0.58[a]	—	—	—	—	—
m_s	(10^{-4} kg)	2.96[a]	1.05[a]	1.53[a]	5.0	5.0	5.0	5.0	5.0
V_R	(10^{-4} m^3)	4.00[a]	4.50[a]	3.50[a]	5.0	5.0	5.0	5.0	5.0
D_{eff}	(10^{-10} m^2/s)	5.29[a]	35.5[a]	5.29[a]	5.0	5.0	5.0	5.0	5.0
k_ℓ	(10^{-4} m/s)	6.9[b]	5.4[b]	0.04[b]	—	13	13	13	13
R	(10^{-4} m)	6.10[b]	3.90[a]	2.31[a]	2.50	2.50	2.50	2.50	2.50
K_F	(m^{3n}/kg^n)	1.93[a]	2.90[a]	1.93[a]	5.55	1.15	2.31	5.55	13.3
n		0.69[a]	0.53[a]	0.69[a]	0.75	0.30	0.50	0.75	1.0
V	(10^{-8} m^3)	33.3[a]	33.2[a]	3.23[a]	1.79	1.79	1.79	1.79	1.79
Q_i	(10^{-3} kg/kg)	76.5[a]	313[a]	23.5[a]	400	400	400	400	400
X_i	(10^{-6} kg/m^3)	212[b]	38.6[b]	24.4[b]	50	5.0	5.0	5.0	—
μ_{max}	(10^{-4}/s)	1.02[b]	1.04[b]	0.47[b]	1.11	1.11	1.11	1.11	1.11
Y	(kg/kg)	0.93[a]	0.83[b]	1.06[b]	0.80	0.80	0.80	0.80	0.80
K_s	(10^{-5} kg/m^3)	4.0[a]	4.0[a]	4.0[a]	4.00	4.00	4.00	4.00	4.00
ε	(m^3/m^3)	0.78[a]	0.71[a]	0.78[a]	0.78	0.78	0.78	0.78	0.78
ρ_s	(10^3 kg/m^3)	1.24[a]	1.08[a]	1.24[a]	1.24	1.24	1.24	1.24	1.24

centrations and a moving average method was applied to calculate the results in Figure 3B. In addition to these calculations, model calculations are given in Figure 3B.

Experiments similar to those with XAD7 were performed with preloaded XAD4 resins and results are shown in Figure 4. At the end of the experiments with the XAD4 resins colorization was also observed, but to a larger extent compared to the tests with XAD7. Here the resins were colored dark brown. The dissolved naphthalene concentration and biomass concentration were calculated according to the mathematical model and, in addition, the residual mass fraction of the naphthalene still present in the particle at a certain moment was given. For this purpose, the residual mass in the particle was calculated by multiplication of the dissolved naphthalene concentration in the pores of the particle and the concentration of sorbed naphthalene by the volume of the shells that were defined for the numerical evaluation. The mass fraction was simply computed by dividing the actual mass in the particle by the initial mass.

To illustrate the effect of external mass-transfer limitations, combined desorption and biodegradation tests were performed at low mixing rates (Sh = 1.7) and the results are shown in Figure 5. In this experiment, bacteria were added to the reactor liquid at the start of the test and the biodegradation capacity was assumed to be negligible in the first 8 h because of the low biomass concentration that was present initially. Two types of model calculations were performed: the parameters were adjusted to optimize the description of the experimental data by the model and the situation was simulated in which external mass transfer is negligible (at a high Biot number). The parameter values are given in Table 3. Additionally, simulations have been performed on a hypothetical system (Table 3) in which the external resistances have been varied over a range of mixing conditions (e.g., Sherwood numbers; Fig. 6). In this

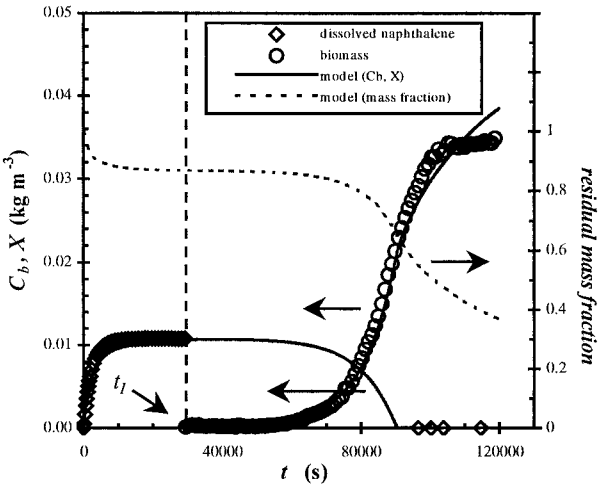

Fig. 4. Desorption of naphthalene from XAD4 particles (710–850 μm) and the subsequent biodegradation by *Pseudomonas* 8909N. Symbols indicate experimental data and drawn lines are model calculations. The vertical dashed line indicates the moment of inoculation (t_l). The mass fraction of naphthalene present in the particle is calculated in time.

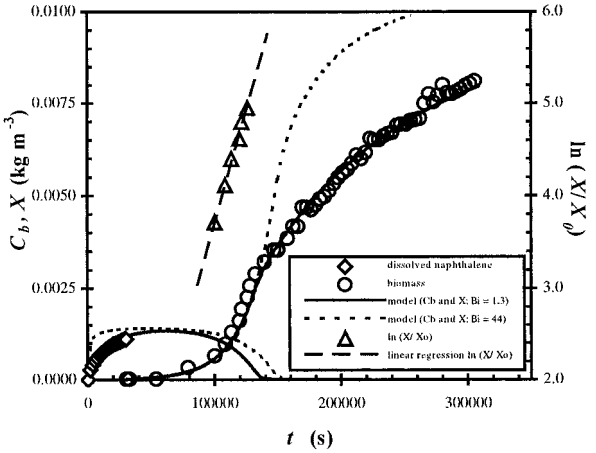

Fig. 5. Desorption from XAD7 (425–500 μm) and simultaneous biodegradation (t_l = 0) of desorbed naphthalene at low mixing conditions (Sh = 1.7) by *Pseudomonas* 8909N. Symbols represent experimental data and the drawn lines are model calculations for the bulk liquid naphthalene concentration (C_b) and the biomass concentration (X). The dotted lines (for C_b and X; Bi = 44) are calculated for the case when external mass-transfer resistances would have been negligible. The conditions and model parameters are given in Table 3.

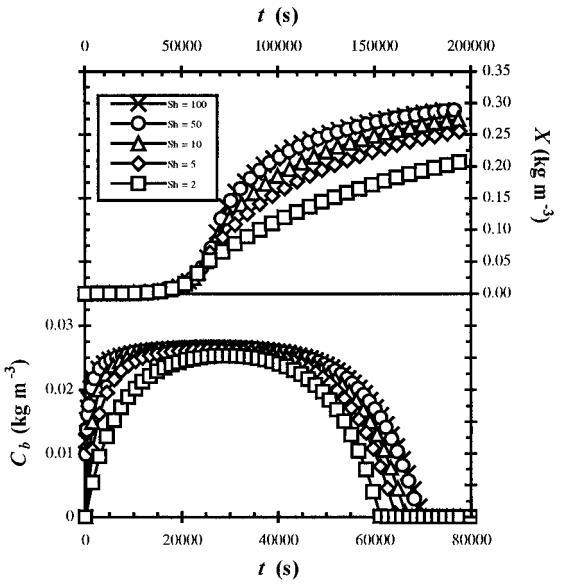

Fig. 6. Model simulations to illustrate the effect of external mass-transfer limitations on the desorption of naphthalene (C_b) from porous particles and the subsequent biodegradation by the bacteria (X).

simulated biodegradation experiment the mass-transfer coefficient was very low and, therefore, biodegradation in the boundary layer might become important. On the basis of Equation 26 a Hatta number of 0.87 was calculated at the highest biomass concentration.

An important feature of the current modeling is the combination of the application of Monod kinetics for the description of the bacterial growth and substrate conversion (e.g., naphthalene) and the use of the nonlinear Freundlich isotherm to describe the sorption of naphthalene to the porous solids. To investigate the effect of the constant n in the Freundlich isotherm and the initial biomass concentration (X_0) on the biodegradation of naphthalene, several calculations were performed (Fig. 7A). In this figure, the mass fraction of naphthalene present in the particle and the biomass concentration are given. Figure 7A shows that a decrease in the value of the Freundlich constant n results in an increased period necessary for removal of a certain mass fraction from the solid. The value of the overall effective diffusion coefficient (D^o_{eff}) was expected to possibly be responsible for this effect. Therefore, the value of this parameter was evaluated as a function of the elapsed time in the simulations of Figure 7A (at $r = 0.5R$) and as a function of the dissolved naphthalene concentration (Fig. 7B).

DISCUSSION

Sorption isotherms

In agreement with earlier experiments in which sorption isotherms of naphthalene on XAD4 and XAD7 resins were determined, nonlinear sorption behavior was observed (XAD4: $n = 0.40$; XAD7: $n = 0.68$; [7]). The XAD4 clearly shows a more strongly nonlinear behavior than the XAD7 resin (a value of $n = 1$ yields a linear isotherm; the more the value of n deviates from unity, the more nonlinear the isotherm is). The Freundlich model has an excellent fit through the experimental data (Fig. 1) and, therefore, other nonlinear models such as, for instance, the Langmuir isotherm were not tested.

Although in most work on the partitioning of hydrophobic

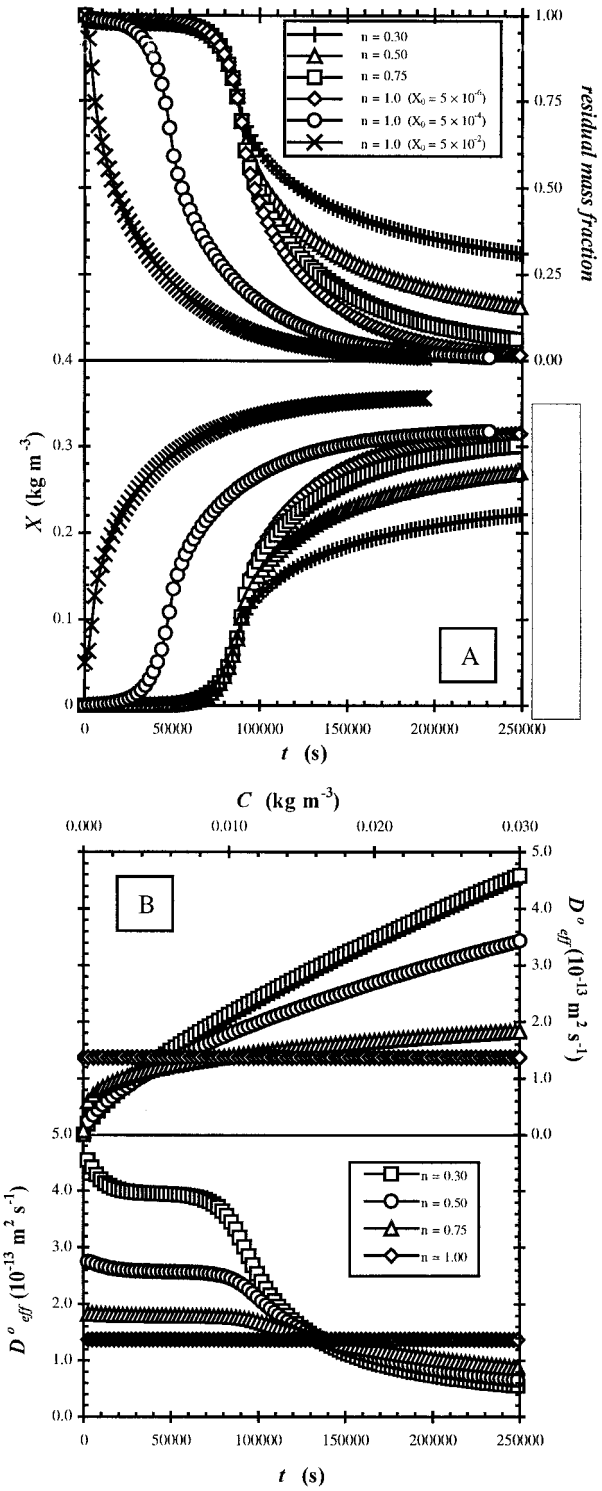

Fig. 7. (**A**) Model simulations showing the effect of the sorption constant n in the Freundlich isotherm on the removal rate of naphthalene from a porous particle (top) and the related biomass formation (bottom). Furthermore, the effect of the initial biomass concentration is illustrated for the linear isotherm ($n = 1$). The initial mass of naphthalene was identical for all simulations (Table 3). (**B**) Model simulations showing the overall effective diffusion coefficient as a function of time (bottom) and as a function of the local naphthalene concentration in the pore liquid of the particles (top). The value of D^o_{eff} was evaluated at $r = 0.5R$.

compounds to soil materials, linear isotherms were applied to describe the data [3,4,8,29,30], several reports exist in which the nonlinear Freundlich isotherm was used [7,31–34]. The suggestion was made that the linear isotherm is applicable to soil material polluted at a low level and that the isotherm becomes nonlinear at relatively high contaminant loadings [30]. The mobility of pollutants in the soil matrix is strongly affected by the type of isotherm used to describe the equilibrium partitioning [31]. However, because of the nonlinearity of the bacterial kinetics, numerical techniques are necessary, and the introduction of another nonlinear process therefore is a marginal effort.

Mass-transfer parameters

The dynamic adsorption and desorption experiments at different mixing conditions clearly show that quantification of the external transfer resistances as a function of reactor hydrodynamics is important when the intraparticle diffusion is studied (Fig. 2). The values of the impeller Reynolds number indicate that the flow is always turbulent in the vicinity of the impeller [24], but laminar regions may exist at certain locations in the reactor at the low mixing speeds. This is supported by the low Sherwood numbers ($Sh \sim 2$ at impeller speeds [S_i] below 0.8/s; data not shown) that were calculated on the basis of the mass transfer coefficients. From Equation 15, the value of the Sherwood number becomes 2 at very low relative velocities of the particle to the fluid.

The values of the effective diffusion coefficients show that the diffusion of naphthalene in the XAD7 matrix is hindered by the tortuosity and constrictivity effects (Table 2). The matrix factor of 1.22 is within the range of 1.08 to 1.28 of matrix factors that are reported on the basis of theoretical and empirical relations that relate the matrix factor to the matrix porosity ($\varepsilon = 0.78$) [21]. However, the effective diffusion coefficient of naphthalene through the XAD4 matrix is found to exceed the water diffusivity. This suggests that surface diffusion occurs, which is probably caused by the strong hydrophobicity of the XAD4 material [35]. Because reports on the significance of surface diffusivity in soil material are lacking, this material (XAD4) seems to be less attractive as a soil model system. Therefore, no attempts were made to alter the model and incorporate surface diffusion processes.

Desorption and subsequent biodegradation

The single-run tests that were developed in earlier work with solid naphthalene to study the mutual influence on mass-transfer and biodegradation processes [12] are also applicable to the current system with porous sorbents (Figs. 3 and 4). In the first stage of the experiment unambiguously quantifying the mass-transfer processes is possible because biodegradation of the substrate is prevented. After inoculation the bacteria consume the desorbed naphthalene and biomass is generated as a results of this conversion. As long as the dissolved naphthalene concentration is far above the Monod constant (K_s), zero-order growth occurs and an exponential growth phase is observed. The maximum growth rate can be determined from this exponential increase in the biomass concentration and the logarithmic plots in Figures 3A and 5 show the good correlation between the experimental data and the linear relation. When the potential biodegradation capacity exceeds the maximum desorption rate, the dissolved naphthalene concentration drops to a very low value. From that moment onwards, the biodegradation of naphthalene is no longer microbiologically limited but becomes mass-transfer limited.

This can also be deduced from Figure 3B, where the experimental desorption and growth rates are compared with model calculations. In the aseptic desorption phase, the desorption rate decreases from the maximum value at the start of the test to zero when equilibrium is established. When bacteria have been added and start to convert the substrate the concentration of dissolved naphthalene decreases. Hereby, the driving force for transfer of naphthalene from the particles is increased and the desorption rate increases.

At the transition point of exponential growth and mass-transfer–limited growth, the dissolved concentration becomes virtually zero and the desorption rate is maximum. Meanwhile, the average naphthalene concentration in the particle has decreased compared to the initial concentration and the maximum desorption rate is significantly lower than the rate at the start of the test. This is different from the systems with solid naphthalene [12] where the maximum dissolution rate remains constant. Because the biodegradation is mass-transfer limited from the transition point onwards, the desorption rate remains maximal. However, the concentration of naphthalene in the particle decreases and, therefore, the maximum desorption rate also decreases. The growth rate of the bacteria decreases drastically from the maximum value in the exponential growth phase to a very low value when the naphthalene concentration decreases to a level far lower than the Monod constant under mass-transfer–limited conditions. Because the biomass concentration still increases because of the conversion of desorbing naphthalene and the desorption rate decreases in time, the growth rate decreases continuously.

Figures 3A, 4, and 5 illustrate the good agreement between the calculated concentrations of dissolved naphthalene and biomass. However, in Figure 3A, and more pronounced in Figure 4, deviations occur between the experimental biomass concentration and the model prediction for this concentration. These experiments were terminated because the decline in the slope of the biomass curve was explained as the depletion of naphthalene from the XAD particles. However, the model calculations show that a considerable amount of naphthalene is still present in the particles at the termination of the tests. In both the experiments with XAD7 and XAD4 biomass or metabolites (or both) were observed to be sorbed to the surface of the Amberlite resins. Given the above-mentioned differences between experimental biomass concentrations and model predictions, significant sorption of biomass to the hydrophobic resins might occur. This was reported earlier [7] and *Pseudomonas* 8909N is known to attach to hydrophobic surfaces [13]. Analysis of whether this attachment affects the analysis of the biomass concentration and whether the mass transfer of naphthalene is influenced might be interesting in future work.

The model prediction for the desorption of naphthalene from the XAD7 particles in the fraction $2{,}360 < d_p < 1{,}000$ μm was observed initially to be poor when an average particle radius (R) of 840 μm was used. Furthermore, a yield of 1.2 kg/kg was determined, which is not a realistic value. Given the wide range of particle diameters in this fraction and the fact that the product specifications of the XAD7 indicate a diameter range of 850 to 250 μm (20–60 mesh), a smaller average radius was assumed to be reasonable. Therefore, a yield of 0.93 kg/kg was assumed, which was determined earlier [12], and the particle radius (R) was optimized and determined

at 610 μm. This clearly stresses the importance of narrow sieve fractions during the preparation of the material.

Although the effective intraparticle diffusion coefficient was determined in several separate adsorption and desorption experiments and was a fixed parameter in the description of the biodegradation experiments, optimizing this parameter in the aseptic phase of the experiment is possible. External mass-transfer resistances must then be assured to be negligible by sufficient mixing. Although the value of the mass-transfer coefficient was optimized in the first part of the experiments, this was only important in the test described in Figure 5, where external resistances limited the rate of naphthalene release. In Figure 3A and B, intraparticle diffusion was rate-limiting for the transfer of naphthalene from the particles to the mixed bulk, as indicated by Biot numbers of 1.6×10^3 and 46, respectively.

The effect of the external resistances is illustrated in Figures 5 and 6. Figure 5 shows the biodegradation of naphthalene, desorbing from XAD7 particles, at low mixing intensities. Although the model calculations show excellent agreement with the experimental data, this situation is not optimal. The porous sorbents were intended to function as a matrix from which slow diffusion of the pollutant occurs. However, model calculations at higher mixing conditions ($Bi = 44$) show that intraparticle mass transfer limits the biodegradation only for a short period (from $t = 1.27 \times 10^5$ s onwards). However, by choosing larger particles (Fig. 3A) this problem can be circumvented.

The simulations that are shown in Figure 6 are calculated with the same value for the effective diffusion coefficient. In fact, the properties of the hypothetical sorbents are almost identical to those of XAD7, to increase the relevance to the current experimental systems. However, in real soil systems porosities (ε) will be much lower and this will cause a strong decrease in the effective diffusion coefficient (Eqn. 3). Furthermore, relative velocities of soil aggregates compared to the fluid will most likely be higher because of larger differences between the particle density and liquid density. The importance of external diffusion limitations therefore will be less pronounced.

The simulations that have been performed to illustrate the effect of the Freundlich sorption constant n (Fig. 7A), clearly demonstrate that deviation from the linear isotherm causes longer biodegradation periods necessary to reduce the contaminant concentration in the particle to certain levels (at equal initially sorbed concentrations [Q_i]). From Equation 5 and Figure 7B, the value of the overall effective diffusion coefficient can be deduced to decrease with a decreasing dissolved naphthalene concentration. This results in lower desorption rates from the particles and consequently in lower biomass formation rates in the mass-transfer–limited part of the simulation. Even in the case of a linear isotherm ($n = 1.0$) the overall effective diffusion coefficient is orders of magnitude lower than the effective diffusion coefficient. This is the reason for the relatively slow release of more hydrophobic soil contaminants in comparison to pollutants that show less sorption to the soil material. In most studies on the sorption of pollutants to soil material, the sorption constant is related to the octanol–water partitioning coefficient of the compound. This quantity is a measure of the hydrophobicity and the interactions with the soil organic matter have been shown to be proportional to this parameter [30].

The calculation at different initial biomass concentrations indicates that the microbiologically limited phase can be shortened by altering the biological parameters. In fact, the kinetically limited phase can be prevented if the potential biodegradation capacity exceeds the maximum desorption rate. In that situation, bioremediation periods can simply be calculated on the basis of a zero bulk liquid concentration when sorption is described by a linear isotherm ($n = 1.0$) [36]. However, as the biomass formation rate becomes zero order at microbiological limited conditions and the desorption rate is limited to a certain maximum value, mass-transfer–limited conditions can be expected eventually to be inevitable. The sufficient supply of other nutrients (e.g., oxygen, nitrogen) is of course a prerequisite to achieve zero-order biodegradation.

CONCLUSIONS

The purpose of this work was to validate a mechanistic model that incorporates both external and intraparticle mass-transfer processes, nonlinear sorption, and nonlinear biological degradation kinetics. The foregoing has showed that the model can adequately describe the sorption, mass transfer and biodegradation processes of naphthalene, initially sorbed in a porous particle. Because the model parameters can all be determined seperately, a mechanistic framework is available with which predictions can be made about the behavior of hydrophobic soil pollutants in systems with nonlinear sorption and Monod bacterial kinetics.

The use of synthetic model soil matrices eliminates the soil heterogeneity that complicates the research for the rate-limiting processes in the biodegradation of PAHs and other hydrophobic soil pollutants. Because the Amberlite resins possess well-defined and constant properties, validation of the model was possible and experimental results were reproducible. For instance, the size of the model soil particles was within defined limits, which is often a problem in real soil slurries. Furthermore, the particles have homogeneous properties, which is not the case for real soil particles wherein heterogeneities occur at all scales. The use of naphthalene as a model PAH is very convenient because the time scales of the experiments are short and analytical difficulties are prevented.

However, the application of these types of soil model systems has drawbacks. In general, two types of disadvantages occur. The occurrence in model matrices of processes that are absent in real soil systems is undesirable. The surface diffusion of naphthalene in the XAD4 resins and the possible sorption of biomass to the Amberlite resins are examples of such processes. However, with respect to the latter, it must be stressed that the major part of the soil biomass is attached to particulate matter. On the other hand, relevant processes for natural systems possibly are impossible to mimic in artificial systems. The formation of bound residues or the aging of pollutants in the soil organic matter are important processes that cannot be simulated in the current model system [37,38]. However, some interesting reports exist on the use of humus-coated silica gels to predict the environmental fate of hydrophobic contaminants [39]. Provided that the properties are reasonably reproducible, these might be soil model systems that will overcome some of the disadvantages of the present system. In addition, the partitioning characteristics will be similar to those of real soil organic matter.

REFERENCES

1. Wilson SC, Jones KC. 1993. Bioremediation of soil contaminated with polynuclear aromatic hydrocarbons (PAHs): A review. *Environ Pollut* 81:229–249.

2. Brusseau ML, Jessup RE, Rao PSC. 1991. Nonequilibrium sorption of organic chemicals: Elucidation of rate-limiting processes. *Environ Sci Technol* 25:134–142.
3. Chung GY, McCoy BJ, Scow KM. 1993. Criteria to assess when biodegradation is kinetically limited by intraparticle diffusion and sorption. *Biotechnol Bioeng* 41:625–632.
4. Connaughton FC, Stedinger JR, Lion LW, Shuler ML. 1993. Description of time-varying desorption kinetics: Release of naphthalene from contaminated soils. *Environ Sci Technol* 27:2397–2403.
5. De Jonge H. 1996. Sorption, bioavailability and mineralization of hydrocarbons in contaminated soils. PhD thesis. University of Amsterdam, Amsterdam, The Netherlands.
6. Guerin WF, Boyd SA. 1992. Differential bioavailability of soil-sorbed naphthalene to two bacterial species. *Appl Environ Microbiol* 58:1142–1152.
7. Volkering F. 1996. Bioavailability and biodegradation of polycyclic aromatic hydrocarbons. PhD thesis. Agricultural University of Wageningen, Wageningen, The Netherlands.
8. Wu S, Gschwend PM. 1986. Sorption kinetics of hydrophobic organic compounds to natural sediments and soils. *Environ Sci Technol* 20:717–725.
9. Crocker FH, Guerin WF, Boyd SA. 1995. Bioavailability of naphthalene sorbed to cationic surfactant-modified smectite clay. *Environ Sci Technol* 29:2953–2958.
10. Darbyshire JF, Chapman SJ, Cheshire MV, Gauld JH, McHardy WJ, Paterson E, Vaughan D. 1993. Methods for the study of interrelationships between micro-organisms and soil structure. *Geoderma* 56:3–23.
11. Harms H. 1996. Bacterial growth on distant naphthalene diffusing through water, air, and water-saturated and non-saturated porous media. *Appl Environ Microbiol* 62:2286–2293.
12. Mulder H, Breure AM, Van Andel JG, Grotenhuis JTC, Rulkens WH. 1998. Influence of hydrodynamic conditions on naphthalene dissolution and subsequent biodegradation. *Biotechnol Bioeng* 57:145–154.
13. Mulder H, Breure AM, Van Honschooten D, Grotenhuis JTC, Van Andel JG, Rulkens WH. 1998. Effect of biofilm formation by *Pseudomonas* 8909N on the bioavailability of solid naphthalene. *Appl Microbiol Biotechnol* 50:277–283.
14. Scow KM, Alexander M. 1992. Effect of diffusion on the kinetics of biodegradation: Experimental results with synthetic aggregates. *Soil Sci Soc Am J* 56:128–134.
15. Dexter AR. 1988. Advances in characterization of soil structure. *Soil Tillage Res* 11:199–238.
16. Emerson WW, Foster RC, Oades JM. 1986. Organo-mineral complexes in relation to soil aggregation and structure. *Soil Sci Soc Am J* 17:521–547.
17. Kay BD. 1990. Rates of change of soil structure under different cropping systems. *Adv Soil Sci* 12:1–51.
18. Waters AG, Oades JM. 1991. Organic matter in water-stable aggregates. In Wilson WS, ed, *Advances in Soil Organic Matter Research*. Royal Society of Chemistry, Cambridge, UK, pp 163–174.
19. Kleijntjens R. 1991. Biotechnological slurry process for the decontamination of excavated polluted soils. PhD thesis. Technical University of Delft, Delft, The Netherlands.
20. Bird RB, Stewart WE, Lightfoot EN. 1960. *Transport Phenomena*. John Wiley & Sons, New York, NY, USA.
21. Van Brakel J, Heertjes PM. 1974. Analysis of diffusion in macroporous media in terms of a porosity, a tortuosity and a constrictivity factor. *Int J Heat Mass Transfer* 17:1093–1103.
22. Ball WP, Roberts PV. 1991. Long-term sorption of halogenated organic chemicals by aquifer material. 2. Intraparticle diffusion. *Environ Sci Technol* 25:1237–1249.
23. Levins DM, Glastonbury JR. 1972. Application of Kolmogoroff's theory to particle–liquid mass transfer in agitated vessels. *Chem Eng Sci* 27:537–543.
24. Perry RH, Chilton CH, Kirkpatrick SD. 1963. *Chemical Engineers' Handbook*. McGraw-Hill, New York, NY, USA.
25. Schlegel HG. 1981. *Allgemeine Mikrobiologie*. Thieme Verlag, Stuttgart, Germany.
26. Press WH, Teukolsky SA, Vetterling WT, Flannery BP. 1992. *Numerical Recipes in Fortran: The Art of Scientific Computing*. Cambridge University Press, Cambridge, UK.
27. Foo SC, Rice RG. 1979. Sorption equilibria and rate studies on resinous retardation beads. 2. Rate studies. *Ind Eng Chem Fundam* 18:68–75.
28. Volkering F, Breure AM, Sterkenburg A, Van Andel JG. 1992. Microbial degradation of polycyclic aromatic hydrocarbons: Effect of substrate availability on bacterial growth kinetics. *Appl Microbiol Biotechnol* 36:548–552.
29. Chiou CT, McGroddy SE, Kile DE. 1998. Partition characteristics of polycyclic aromatic hydrocarbons on soils and sediments. *Environ Sci Technol* 32:265–269.
30. Karickhoff SW. 1981. Semi-empirical estimation of sorption of hydrophobic pollutants on natural sediments and soils. *Chemosphere* 10:833–846.
31. Hinz C, Gaston LA, Selim HM. 1994. Effect of sorption isotherm type on predictions of solute mobility in soil. *Water Resour Res* 30:3013–3021.
32. Huang W, Weber WJ. 1997. A distributed reactivity model for sorption by soils and sediments. 10. Relationships between desorption, hysteris, and the chemical characteristics of organic domains. *Environ Sci Technol* 31:2562–2569.
33. Liu KH, Enfield CG, Mravik SC. 1991. Evaluation of sorption models in the simulation of naphthalene transport through saturated soils. *Ground Water* 29:685–692.
34. Weber WJ, Miller CT. 1988. Modeling the sorption of hydrophobic contaminants by aquifer materials—I. *Water Res* 22:457–464.
35. Komiyama H, Smith JM. 1974. Intraparticle mass transport in liquid-filled pores. *AIChE J* 20:728–734.
36. Mulder H, Breure AM, Rulkens WH. 1998. Bioremediation potential as influenced by the physical status of PAH pollutants. *Proceedings*, Contaminated Soil 1998, Edinburgh, UK, May 17–21, pp 133–142.
37. Eschenbach A, Kästner M, Bierl R, Scheafer G, Mahro B. 1994. Evaluation of a new, effective method to extract polycyclic aromatic hydrocarbons from soil samples. *Chemosphere* 28:683–692.
38. Hatzinger PB, Alexander M. 1995. Effect of aging of chemicals in soil on their biodegradability and extractability. *Environ Sci Technol* 29:537–545.
39. Szabo G, Guczi J. 1995. Examination of silica-salicyclic acid and silica-8-hydroxyquinoline HPLC stationary phases for estimation of the adsorption coefficient of soil for some aromatic hydrocarbons. *Chemosphere* 30:1717–1727.
40. Gustafson KE, Dickhut RM. 1994. Molecular diffusivity of polycyclic aromatic hydrocarbons in aqueous solution. *J Chem Eng Data* 39:281–285.